Nanoparticles designed from low pressure plasma as model for astrophysical dust clouds

Ilija Stefanovic, Eva Kovacevic, Johannes Berndt, Yvonne Pendleton, Jörg Winter

Nanoparticles designed from low pressure plasmas as identification tool for astrophysical observations

Ilija Stefanović, Eva Kovačević, Johannes Berndt, Yvonne Pendleton, and Jörg Winter

[1)] Institute of Experimental Physics II, Ruhr-University Bochum, D-44780 Bochum, Germany, is@ep2.rub.de.

[2)] Institute of Physics, POB 57, 11001 Belgrade, Serbia and Montenegro.

[3)] NASA Ames Research Center, Mail Stop 245-3, Moffett Field, CA 94035, USA.

PAC's numbers:
81.05 Uw,

Abstract

In this paper we analysed morphology and chemistry of carbonaceous dust particles proposed as a candidate analog material for dust in diffuse interstellar media. The particles were polymerised in a low pressure capacitively coupled radio-frequency discharge in mixtures of argon/acetylene and helium/acetylene. Infrared absorption spectra of our dust particles reveal the strong presence of aliphatic features, both stretching and bending, very similar to astronomical data from diffuse interstellar media. The comparison between the infrared spectra obtained in argon and in helium as buffer gas reveals in the case of helium a strong presence of C=C double bonds (skeletal modes). The presence of these skeletal modes is clearly visible through the broad absorption feature at 1600 cm^{-1}.

1. Introduction

Studies on the formation of dust particles in low temperature reactive plasmas were triggered by their negative effects in plasma processing of microelectronic devices where they were recognized as killer particles. On the other hand plasma grown nanoparticles can be used as efficient catalysts, in bio-medical applications as transporters of drugs to the target tissue or they can be incorporated in thin films where they improve film quality and film function.

Another important field where dust plays a specific role is the astrophysics. Dust particles are often found in diffuse and dense interstellar media (ISM) (Sandford et al. 1991, Pendleton et al. 1994, Whittet et al. 1997), circumstellar shells (Gauger, Sedlmayr, and Gail, 1990), dark interiors of molecular clouds (Neckel and Staude, 1987), stellar envelopes (Jura 1990), nova ejecta (Gehrz et al., 1998), the outflow of red giant stars, proto-planetary nebulae (Cassinelli 1979, Woolf and Ney 1969, Chiar et al. 1998), and the interstellar medium of other galaxies (Spoon et al. 2003). Even though interstellar gas dominates the mass balance by a factor 100, dust plays an important role in the ISM. In particular, interstellar dust regulates star formation, catalyzes molecule production and reprocesses UV and optical radiation.

The C-H stretch vibration of aliphatic hydrocarbons located at a wavelength around 3.4 μm is used to trace carbonaceous dust particles. This absorption feature at 3.4 μm has been already detected by more than two dozen sightlines through diffuse ISM in our galaxy as well as in the rest frame spectra of several nearby galaxies (Butchart et al. 1986; Sandford et al. 1991, Pendleton et al. 1994, Pendleton et al. 1997, Whittet et al. 1997, Adamson et al. 1990; Rawlings, Adamson and Whittet 2003, Marco and Brooks 2003, Bridger, Wright and Geballe 1994; Mizutani, Suto and Maihara 1994; Wright et al. 1996; Imanishi et al. 1997; Imanishi 2000a,b; Imanishi and Dudley 2000; Imanishi, Dudley and Maloney 2001; Imanishi 2002, 2003; Marco and Brooks 2003; Risaliti et al. 2003). The 3.4 μm band is accompanied by two weak bending mode bands at longer wavelengths, which occur at 6.8 and 7.2 μm (Chiar et al. 2000).

Comparisons of IR spectra obtained from laboratory residues and astrophysical observations provide clues to the origin of the carbonaceous ISM material. Recently we proposed a new candidate for a carbonaceous interstellar dust analog based on the dust growth in a capacitively coupled the radiofrequency discharge in argon/acetylene mixtures [Kovacevic submitted]. The particles are analyzed in-situ during their growth by means of a sensitive multi-pass Fourier Transformed Infrared (FTIR) technique. This in-situ diagnostic enables us to investigate the formation of the particles in a well-defined environment. Thus, the

influence of oxygen and nitrogen as well as different buffer gases, such as argon and helium, on the IR spectra can be studied in detail, simply by careful designing of the gas mixture.
This candidate was tested according the criteria established in the literature (Pendleton, Allamandola).
In this paper we review some of the main characteristics of our analog candidate, including an analysis of the particles by means of transmission electron microscopy (TEM), a study of the particle growth-rate, and a detailed analysis of the IR spectrum of the particles. We analyze the spectral region of 1700 cm^{-1} to 500 cm^{-1} which contains information on hydrocarbon C-H deformation bands (1450 cm^{-1} and 1370 cm^{-1}) and numerous aromatic and cyclic groups. The 2000 cm^{-1} – 1250 cm^{-1} features prove critical to any spectral analysis of carbonaceous materials. Beside that, we study the influence of the different carrier gases (argon and helium) to the IR absorption of the dust and its composition.

2. Experimental set-up

The investigations were performed in a capacitively-coupled parallel plate reactor, symmetrically driven by radio frequency power (RF) at 13.56 MHz. The electrode system consists of two plain stainless steel electrodes, 30 cm in diameter and separated by 8 cm. The reactor was operated at room temperature, with gas mixtures of acetylene and argon and acetylene and helium, respectively. The continuous gas flow was controlled by mass flow controllers. The total gas pressure was about 0.1 mbar. The characteristic pumping speed of the system gives a mean gas residence time of about 1 min. The applied RF power was 10-50 W, measured before the match-box. The details of the experimental set-up details can be found in our previous papers (Kovačević et al. 2003).
The technique of Infrared (IR) absorption spectroscopy was used to monitor the formation of dust particles inside the plasma volume. The particles are growing in the plasma bulk between the two electrodes due to homogeneous gas-phase nucleation. Since the particles in the plasma are negatively charged they are confined in the plasma bulk due to the action of the electric force: they levitate between the electrodes without touching the electrodes during their lifetime (as previously described in Kovačević et al 2003, Berndt et al 2003). The IR beam from the commercial Bruker FTIR spectrometer was directed through KBr windows in the plasma chamber and was focused with an off-axis gold mirror onto an external liquid-nitrogen-cooled mercury-cadmium-telluride detector. By means of a multi-pass technique we were able to change the optical path length in the plasma from 0.6 meters (2 passes through

plasma reactor) to 7.2 meters (24 passes). The cross section of the beam has a radius of 1 cm. Due to the reflections of the beam in the multi-pass reflection cell the final area monitored by the IR has a size of 2cm × 5cm.

The formation of thin films on windows and mirrors, which could lead to an unwanted absorption of the IR beam, is avoided by using an argon (optionally nitrogen) gas shower.

One single IR scan lasts up to one second. Usually we integrate over 50 single scans in order to achieve high resolution in the spectra. We followed the time evolution of the IR signal by measuring full FTIR spectra with a time resolution of 1 min.

During the measurement there is a significant deposition of DLC films on the electrodes and discharge chamber walls. Therefore we cleaned the discharge chamber after each measurement session with oxygen plasma. After this treatment, the plasma vessel was pumped for several hours. The residual gas pressure was $6 \cdot 10^{-6}$ mbar.

3. Experimental results

3.1 Dust morphology and growth rate

The particles were collected for different plasma processing times on a silicon wafer which was located on the lower electrode. They were investigated by means of a Scanning and Transmission Electron Microscopy (SEM and TEM).

Figure 1 shows an example of a SEM picture. As can be seen the size distribution of the particle radius is rather narrow. Measured radii versus plasma-processing time are shown on the Fig. 2. From a least-square fit we estimate a particle growth rate of 23 nm/min (dashed line on Fig. 2). This growth velocity cannot be extrapolated to the first minutes after the plasma was switched on because nonlinear processes of coagulation of primary particles take place in the very beginning of the dust growth process.

Figure 3a shows a TEM picture of a cauliflower shaped particle with loose cones and fractal surface texture which was collected 8 minutes after the ignition of the plasma. The particle diameter is about 250 nm. It is known ((Haaland et al. 1994; Garscadden et al. 1994) that such spheroid grains are characteristic for homogenous growth in the plasma. Grains with similar spheroid shape and surface texture have been observed from submicron to sub millimetre size in several kinds of dusty plasmas, for example dust grown in helium plasma by sputtering from graphite electrodes (Garscadden et al. 1994). According to literature

(Haaland et al. 1994) such a microstructure is explained as growth by ballistic deposition rather than diffusion limited aggregation.

A closer look to the particle shows an amorphous structure of the particle surface (Fig. 3b). Due to the constrictions of our TEM, one can not uniquely decide weather the particle nucleus is crystalline or not, or whether there are possible crystalline islands.

The diffraction pattern (Fig. 4) suggests that the material is essentially amorphous due to the diffuse hallo and ring pattern. A crystalline material would be characterized by sharp concentric rings. Due to the limited resolution we can presently not exclude, however, a small fraction of nano-crystalline inclusions in the otherwise amorphous matrix.

3.2 The role of the helium as the carrier gas on the dust chemistry

The most prominent feature observed in the diffuse interstellar media is the 3.4 μm feature, revealing the aliphatic nature of the particles (the band position corresponds to CH_3 and CH_2 stretching vibrations). Our analog-candidate have an IR spectrum comparable with the astronomical observations, for example near infrared spectral observations of the 3.4 μm absorption band detected in DISM dust toward Cygnus OB2 No.12 (IR bright background source; Sandford et al. 1991) and the Galactic Center (Pendleton et al. 1994), and the mid-infrared absorption spectra of DISM dust observed towards the Galactic Center using the Infrared Space Observatory (Chiar et al. 2000) (see fig 5 for our experimental results and Pendletonand and Allamandola 2002 for a review of the IR spectra from analog and interstellar data).

Here we compare the IR spectra of dust particles gained from acetylene as precursor in two different carrier gasses, He and Ar. Fig. 6 shows a comparison of two spectra obtained for the same dust growth phase (normalization in the figure on the 2926 cm^{-1} line).

The substructures in the dominant 2940 cm^{-1} (3.4 μm) feature are identified as: $-CH_3$ symmetric stretching (2870 cm^{-1} / 3.48 μm), $-CH_3$ antisymmetric (2960 cm^{-1} / 3.38 μm), and antisymmetric $-CH_2-$ stretching (2926 cm^{-1} / 3.42 μm) (Sandford et al. 1991). Y. Bounouh et al. report in addition on the existence of symmetric CH_2 vibrations being responsible for the longer tail of the whole feature towards low frequencies.

The relative strengths of these sub features imply a $-CH_2/-CH_3$ ratio of ~2.5, characteristic for short-chain hydrocarbons (Sandford et al. 1991, Pendleton et al. 1994, Pendleton and Allamandola 2002). The details of the profile are explained in the literature, including the

influence of perturbing electronegative groups that can blend some of the sub features seen in normal alkanes (Sandford et al 1991). The strength of the whole feature was lower in helium than in argon, but with a very similar shape (Fig. 6).

The deformation modes which correspond to the stretching vibrations around 3.4 μm are placed in the region 1300-1500 cm^{-1}. In both the helium and the argon case we can observe a doublet of sharp peaks at 1450 cm^{-1} and 1375 cm^{-1} (see figure 7a). This doublet confirms the aliphatic character of the dust particles identified by: essentially out-of-phase bending mode (1450 cm^{-1}) and the in-phase bending mode (1375 cm^{-1}, scissors) of CH_3 groups [Ristein et al 1998]. The latter (1375cm^{-1}) component is the only one which does not overlap with other modes, it can be fitted accurately by one Gaussian and can be taken as a signature for the presence of methyl groups (Sokrates, Bounouh, Ristein). Figure 5 shows that the ratio between CH stretching and bending modes differs for the two carrier gases.

The peak centred at 1700 cm^{-1}, can be assigned to carbonyl (C=O) stretching vibrations. Its visibility is due to the higher intrinsic strength of the absorption band associated with C=O stretching mode, which makes even small traces of carbonyl groups (oxygen) detectable.

Another important feature in the spectral region below 1800 cm^{-1} is the band located in the region 1550 – 1600 cm^{-1}. It was shown (Robertson-Ferrari, Valeria) that in the region below 1800 cm^{-1} CC skeleton modes play a significant role in the IR spectra of hydrogenated carbon material. The thesis was proven with H-D substitution experiments (Ferrari 2003, Victoria et al 199?), revealing clearly a CC skeletal region between 1300 – 1400 cm^{-1} and 1550 – 1600 cm^{-1}.

Figure 7b is an insert from Fig. 7a, presenting a comparison of the spectra in the He and Ar case in the region from 1500-1750 cm^{-1}. In the case of the particles grown with argon as carrier gas we can observe the peak at 1600 cm^{-1}, arising as a shoulder on the low frequency tail of the carbonyl feature. This relatively sharp peak must be ascribed to C=C double bond stretching vibrations (Kobayashi, Bonouh, Ferrari, Sokrates), probably of aromatic origin (skeleton modes).

In the case of helium as the carrier gas, this peak is dominant, broad and well defined, it is over blending C=O (now visible only as shoulder on 1600 cm^{-1}) and the strength of the shape is comparable with those of the sp^3 CH_3 doublet. From the width of this feature it is possible to conclude that the C=C bonds are found here in many different configurations, both alkene and aromatic, and that these configurations are probably distorted [Bounouh, Sokrates]. The broadening of this band can come also from overlapping with adjoining sp^2 C-H vibrations [Bounouh]. In the case of the particles grown in Ar matrix, this peak is clearly weaker.

The presence of the peak in this range is characteristic for C=C double bonds only, and can be an indication that there is a fraction of sp^2 C atoms bonded not to H, but only to other C atoms.

The next region of interest is the region of lower energies, with a strong broad maximum centered at 1250 cm^{-1} (see Fig.7a). It is rather difficult to identify peaks in the fingerprint area (1350-900 cm^{-1}) with particular vibrations since the bands may arise here in various ways [Sokrates]. This region is dominated by C-O-C stretching vibrations. Their intensity depends strongly on the presence of oxygen in the bulk of the material which results in our case may be due to water vapor contamination of the reactor. Carbonaceous materials produced from unsaturated precursors like acetylene and ethylene (Kobayashi et al. 1974) are very susceptible to the reactions with oxygen. In the case of double bonds, like –C=C-, the reactions with water, hydroxyl or oxygen lead easily to –C-O-C- formation.

On the other hand C-C skeletal vibrations (mixed sp^2/sp^3 sites) enhanced by coupling with CH group vibrations also appear in this spectral region [Koidl, Colthup, Soki, Ferrari]. These bands s are over blended in our case due to the presence of oxygen contamination.

The absorption region below 1050 cm^{-1} reveals in both spectra clearly well-defined bands. This whole absorption region (if we follow the frequencies till 729 cm^{-1}, the position of the strongest acetylene vibrations) is assigned to H bonded sp^2 C sites. These have both alkene and/or aromatic origin. The strength of those sp^2 bands is again stronger in the case of helium as carrier gas.

4. Conclusions

In this paper we analysed morphology and chemistry of carbonaceous dust particles proposed as a candidate analog material for dust in diffuse interstellar media. The particles were polymerised in a capacitively coupled discharge in mixtures of argon/acetylene and helium/acetylene.

Ex-situ SEM measurements show that the particle growth is essentially monodisperse. The growth velocity, after the first stage of nucleation and coagulation, is about 23 nm/min. Due to the limited resolution of our TEM device we cannot decide at this time whether we have small crystalline structures within our particles. Further investigations with improved TEM resolution shall clear weather the particle nucleus is more crystalline-like or amorphous.

The IR analysis of the particles reveal the significant presence of CH aliphatic bands (both stretching and bending) similar to those obtained from astrophysical observations from diffuse interstellar media (Pedleton and Allamandola).

Although the spectra obtained with different carrier gases do not differ significantly on a first sight, there is an important difference. The spectrum of particles grown in a mixture of helium and acetylene exhibits the presence of carbon double bonds in the material (indication of sp^2 sites). The evidence of C=C skeletal vibrations in spectra obtained with helium is the strong feature arising at 1600 cm^{-1}, which is dominating over the usually strong carbonyl feature. This band is observed also with argon, but significantly weaker. Another indication for the stronger C=C presence in the helium case is the strength of the well-defined bands in the area under 1050 cm^{-1}, the whole region being assigned to H bonded sp^2C sites.

The broad feature with a maximum centred at 1250 cm^{-1} can be in both cases connected with C-O-C stretching vibrations. The presence of water and oxygen impurities was in cases, helium and argon, very low. In the case of helium the C-O-C stretching area is more pronounced than in the Ar case. Since C=C double bonds are highly susceptible for the reactions with oxygen – leading to the –C-O-C- formation – this confirms the higher amount of C=C bonds in the particles polymerised in helium/acetylene mixtures (Kobayashi).

In the case of astrophysical observations, the feature at 1600 cm^{-1} (6.25 μm) was not observed or was very week in the spectra of carbonaceous dust in diffuse ISM.

The explanation of the differences observed in the spectra is out of the scope of this paper and can not be given without a clearer picture on the sp^2 sites concentration and sp^2/sp^3 ratio for the given materials, as well as the characterisation of the plasma conditions, what would be the direction of our further work.

Aknowledgements

The authors kindly acknowledge Dr. R. Neuser for SEM images and Dr. Kristof Somsen for TEM images of our particles. This study is supported by Deutsche Forschungsgemeinschaft within SFB 591 (projects B1 and B5).

References

Adamson, A.J., Whittet, D.C.B., Chrysostomou, A., Hough, J.H., Aitken, D.K., Wright, G.S., and Roche, P.F. 1999, ApJ, 512, 224

Allain, T., Sedlmayr, E., and Leach, S. 1997, AandA, 323, 163

Allamandola, L.J., Tielens, A.G.G.M., and Barker, J.R. 1989, ApJS, 71, 733

Bernatowicz, T.J., Amari, S., Zinner, E.K., and Lewis, R.S. 1991, ApJ 373, L73

Berndt, J., Hong, S., Kovačević, E., Stefanović, I., and Winter, J. 2003, Vacuum V71, 377

Bernstein, M.P., Sandford, S.A., and Allamandola, L.J. 2002, ApJ 542, 894

Bounouh, Y., Thèye, M.L., Dehbi-Alaoui, A., Matthews, A., Stoquert J.P., 1995, Phys. Rev.B, 51, 9597

Butchart, I., McFadzean, A. D., Whittet, D.C.B., Geballe, T.R., and Greenberg J.M. 1986, *A&A***, 154**, L5

Chair, J.E., Tielens, A.G.G.M., Whittet, D.C B, Schutte,W.A.; Boogert, A. C. A., Lutz, D., van Dishoeck, E. F.; Bernstein, M. P. 2000, *ApJ*, **537**, 749

Chair, J.E., Adamson, A.J., Pendleton, Y.J., Whittet, D.C., Caldwell, D.A., and Gibb, E.L. 2002, *ApJ*, **570,** 198

Ferrari, A.C., Rodil, S.E., and Robertson, J., 2003, Phys. Rev. B, 67, 155306-1

Garscadden, A., Ganguly, B., Haaland, P., and Williams, J. 1994, Plasma Sources Sci Technol., 3, 239

Greenberg, J. M., and Li, A. 1996, A and A., 309, 258

Haaland, P.D., Garscadden, A., Ganguly, B., Ibrani, S., and Wiliams, J. 1994, *Plasma Sources Sci. Technol.* **3**, 381

Imanishi, M., Terada, H., Sugiyama, K., Motohara, K., Goto, M., and Maihara, T. 1997, *PASJ*, **49**, 69

Imanishi, M. 2000, *MNRAS*, **313**, 165

Imanishi, M. and Dudley, C. 2000, *ApJ*, **545**, 701

Jura, M. 1990, *ApJ*, **365**, 317

Kobayashi, H., Bell, A.T., and Shen, M. 1974, *Macromolecules*, **7**, 277

Kovačević, E., Stefanović, I., Berndt, J., and Winter, J. 2003, *J. Appl. Phys.,* **93,** 2924

Kovačević, E., Stefanović, I., Berndt, J., Pendleton, Y.J., and Winter, J. 2004, *Ap.J*, submitted

Mennella,V., Brucato, J.R., Colangeli, L., and Palumbo P. 1999, *ApJ* **513**, L71

Pendleton, Y.J., Sandford, S. A., Allamandola, L. J., Tielens, A.G.G.M., and Sellgren, K. 1994, *ApJ*, **437**, 683

Pendleton, Y.J. 1997, *Origins of Life and Evolution of the Biosphere*, **27 (1-3)**, 53

Pendleton, Y.J., Tielens, A.G.G.M., Tokunaga, A.T., and Bernstein, M.P. 1999, ApJ 513, 294

Pendleton, Y.J., and Allamandola, L.J. 2002, *ApJS* **138**, 75

Pendleton, Y. J. 2004, ASP *Conference Series,* **309**, 573 (eds. A.N. Witt, B.T. Draine, and G.C. Clayton, (ASP: San Francisco))

Perrin, J., and Hollenstein, C. 1999, in Dusty Plasmas edited by A. Bouchoule, Wiley and Sons, New York

Praburam, G., and Goree J. 1995, *ApJ*, **441**, 830

Ristein, J. R.T. Stief, Ley, L., and Beyer W., 1998, *J. Appl. Phys*., **84**, 3836

Sandford, S.A., Allamandola, L.J., Tielens, A.G.G.M, Sellgren, K., Tapia, M., and Pendleton, Y.J. 1991, *ApJ*, **371**, 607

Schutte, W.A., Greenberg, J.M., Van Dishoeck, E.F., Tielens, A.G.G.M., Boogert, A.C.A., and Whittet, D.C.B. 1997, *ApandSS*, **255** 1,

Socrates, G. 1980, Infrared Characteristic Group Frequencies: Tables and Charts, Wiley and Sons, New York

Stefanović, I., Kovačević, E., Berndt, J., and Winter, J. 2003, *New J.Phys.,* **5**, 39

Stoykov, S., Eggs, C., and Kortshagen, U. 2001, *J.Phys. D: Appl.Phys.* **34**, 2160

Whittet, D,C,B., Boogert, A.C.A., Gerakines, P.A., Schutte, W., Tielens, A.G.G.M., de Graauw, Th., Prusti, T., van Dishoeck E.F., Wesselius, P.R., and Wright, C.M. 1997, *ApJ*, **490**, 729

Whittet, D. C. B., Pendleton, Y. J., Gibb, E. L., Boogert, A. C. A., Chiar, J. E., Nummelin, A. 2001 *ApJ*, **550**,793

Figure captions:

Figure1: Scanning electron micrograph showing overview of the dust particles collected on the wafer placed on the lower electrode 5 minutes after the growth process started. Particles were growing in Ar:C_2H_2 discharge, by power of 15W and 0.1 mbar pressure.

Figure 2: Close circles present measured radii versus plasma-processing time. Dashed line: the least-square fitting curve. We estimate a particle growth rate of 23 nm/min. Solid line depicted the different slope for the non-linear processes at the beginning of the particle formation.

Figure 3a: TEM picture of the particle grown in Ar:C_2H_2 discharge. The particles were collected 8 minutes after the ignition of the plasma and its diameter is about 250 nm.

Figure 3b: Magnified insert from the figure 3a showing the amorphous structure of the particle surface.

Figure 4: Diffraction pattern of a particle with a diameter of about 250 nm.

Figure 5: Comparison of two IR spectra in the region 600-4000 cm^{-1}. Solid line: spectrum obtained in Ar:C_2H_2 gas mixture, dotted line: spectrum obtained in He:C_2H_2 gas mixture. In both cases input power was 15 W and total pressure 0.1mbar. Spectra were normalized to the strength of the CH stretching feature in the case of Ar:C_2H_2 mixture.

Figure 6: Comparison of IR spectra in the region of CH stretching vibrations: 2750-3200 cm^{-1}. Solid line: spectrum obtained in Ar:C_2H_2 gas mixture, dotted line: spectrum obtained in He:C_2H_2 gas mixture. In both cases input power was 15 W and total pressure 0.1mbar.

Figure 7a: Insert from the Fig. 5, presenting low energy part of the IR spectra, from 1000-1850 cm^{-1}. Solid line: spectrum obtained in Ar:C_2H_2 gas mixture, dotted line: spectrum obtained in He:C_2H_2 gas mixture.

Figure 7b: Comparison of the IR spectra in the region of double bond modes: solid line: spectrum obtained in Ar:C_2H_2 gas mixture, dotted line: spectrum obtained in He:C_2H_2 gas mixture.

Figure 1.

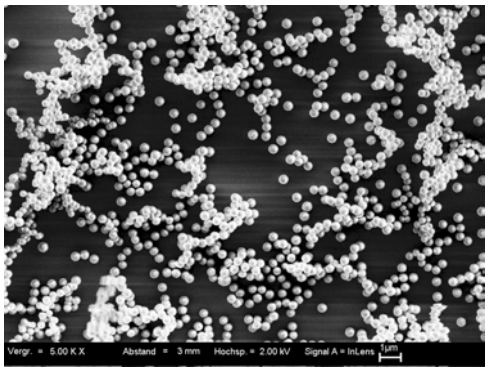

Figure 2

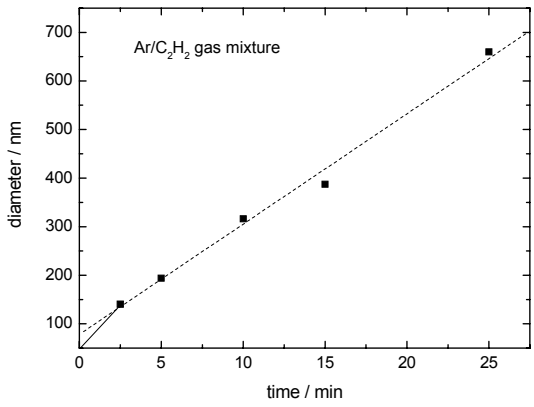
Ar/C2H2 gas mixture
diameter / nm
time / min
700
600
500
400
300
200
100
0
5
10
15
20
25

Figure 3a

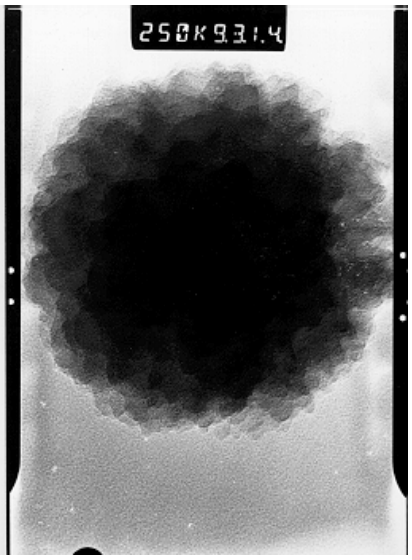

Figure 3b

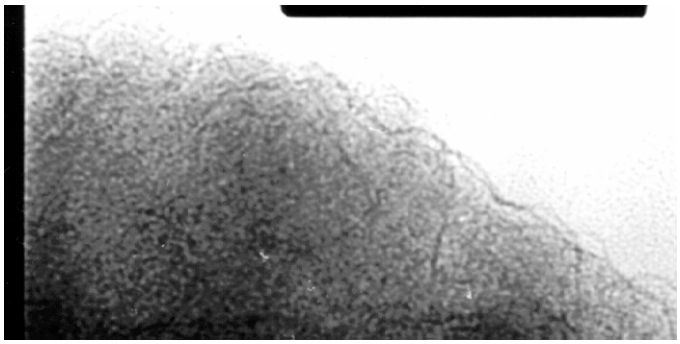

Figure 4

Figure 5

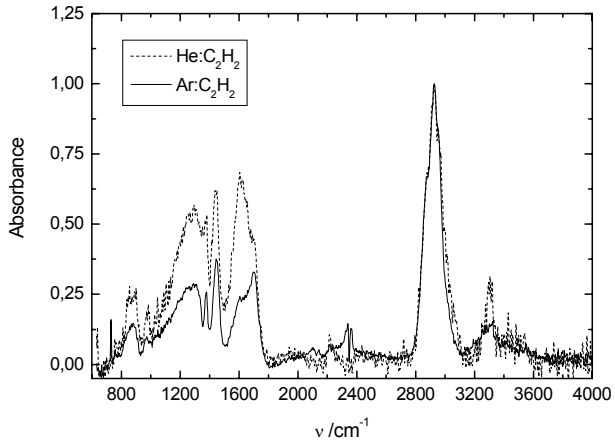
1,25
1,00
0,75
0,50
0,25
0,00
Absorbance
He:C2H2
Ar:C2H2
800
1200
1600
2000
2400
2800
3200
3600
4000
ν /cm-1

Figure 6

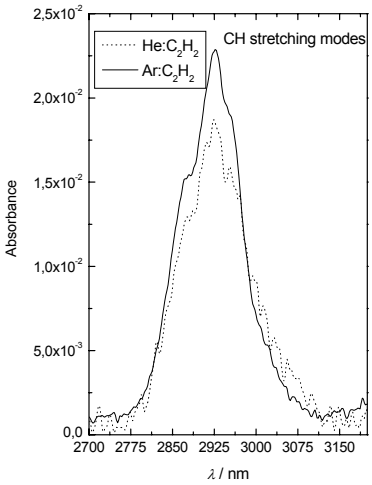
2,5x10-2
2,0x10-2
1,5x10-2
1,0x10-2
5,0x10-3
0,0
Absorbance
He:C2H2
Ar:C2H2
CH stretching modes
2700 2775 2850 2925 3000 3075 3150
λ / nm

Figure 7a

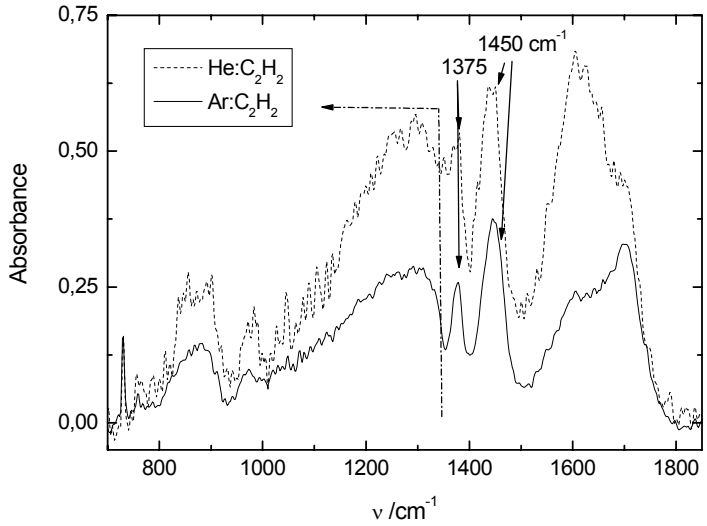
0,75
0,50
0,25
0,00
Absorbance
800
1000
1200
1400
1600
1800
ν /cm-1
He:C2H2
Ar:C2H2
1375
1450 cm-1

Figure 7b

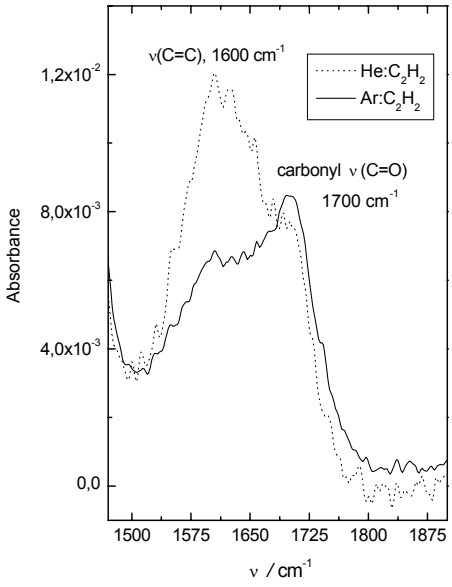
ν(C=C), 1600 cm-1
He:C2H2
Ar:C2H2
carbonyl ν (C=O)
1700 cm-1
Absorbance
1,2x10-2
8,0x10-3
4,0x10-3
0,0
1500
1575
1650
1725
1800
1875
ν / cm-1